# Combined Bezafibrate and Medroxyprogesterone Acetate: Potential Novel Therapy for Acute Myeloid Leukaemia

**Farhat L. Khanim[1], Rachel E. Hayden[1], Jane Birtwistle[1], Alessia Lodi[2], Stefano Tiziani[2], Nicholas J. Davies[1], Jon P. Ride[1], Mark R. Viant[1], Ulrich L. Gunther[2], Joanne C. Mountford[3], Heinrich Schrewe[4,5], Richard M. Green[1], Jim A. Murray[6], Mark T. Drayson[7]ϑ, Chris M. Bunce[1]ϑ***

**1** School of Biosciences, University of Birmingham, Birmingham, United Kingdom, **2** Henry Wellcome Building for Biomolecular NMR Spectroscopy, CRUK Institute for Cancer Studies, University of Birmingham, Birmingham, United Kingdom, **3** Division of Cancer Sciences and Molecular Pathology, University of Glasgow, Glasgow, United Kingdom, **4** Department of Developmental Genetics, Max-Planck Institute for Molecular Genetics, Berlin, Germany, **5** Institute of Medical Genetics, Charité-University Medicine Berlin, Berlin, Germany, **6** Centre for Clinical Haematology, Queen Elizabeth Hospital, Birmingham, United Kingdom, **7** Division of Immunity and Infection, University of Birmingham, Birmingham, United Kingdom

## Abstract

***Background:*** The majority of acute myeloid leukaemia (AML) patients are over sixty years of age. With current treatment regimens, survival rates amongst these, and also those younger patients who relapse, remain dismal and novel therapies are urgently required. In particular, therapies that have anti-leukaemic activity but that, unlike conventional chemotherapy, do not impair normal haemopoiesis.

***Principal Findings:*** Here we demonstrate the potent anti-leukaemic activity of the combination of the lipid-regulating drug bezafibrate (BEZ) and the sex hormone medroxyprogesterone acetate (MPA) against AML cell lines and primary AML cells. The combined activity of BEZ and MPA (B/M) converged upon the increased synthesis and reduced metabolism of prostaglandin $D_2$ ($PGD_2$) resulting in elevated levels of the downstream highly bioactive, anti-neoplastic prostaglandin 15-deoxy $\Delta^{12,14}$ $PGJ_2$ (15d-$PGJ_2$). BEZ increased $PGD_2$ synthesis via the generation of reactive oxygen species (ROS) and activation of the lipid peroxidation pathway. MPA directed prostaglandin synthesis towards 15d-$PGJ_2$ by inhibiting the $PGD_2$ 11β -ketoreductase activity of the aldo-keto reductase AKR1C3, which metabolises $PGD_2$ to 9α11β-$PGF_{2\alpha}$. B/M treatment resulted in growth arrest, apoptosis and cell differentiation in both AML cell lines and primary AML cells and these actions were recapitulated by treatment with 15d-$PGJ_2$. Importantly, the actions of B/M had little effect on the survival of normal adult myeloid progenitors.

***Significance:*** Collectively our data demonstrate that B/M treatment of AML cells elevated ROS and delivered the anti-neoplastic actions of 15d-$PGJ_2$. These observations provide the mechanistic rationale for the redeployment of B/M in elderly and relapsed AML.

**Citation:** Khanim FL, Hayden RE, Birtwistle J, Lodi A, Tiziani S, et al. (2009) Combined Bezafibrate and Medroxyprogesterone Acetate: Potential Novel Therapy for Acute Myeloid Leukaemia. PLoS ONE 4(12): e8147. doi:10.1371/journal.pone.0008147

**Editor:** Michael Goodyear, Dalhousie University, Canada

**Received** June 25, 2009; **Accepted** November 1, 2009; **Published** December 7, 2009

**Copyright:** © 2009 Khanim et al. This is an open-access article distributed under the terms of the Creative Commons Attribution License, which permits unrestricted use, distribution, and reproduction in any medium, provided the original author and source are credited.

**Funding:** Funding was recieved from Leukaemia Research UK and Marie Curie Transfer of Knowledge (ToK) (MOTET). The funders had no role in study design, data collection and analysis, decision to publish, or preparation of the manuscript.

**Competing Interests:** The authors have declared that no competing interests exist.

* E-mail: C.M.Bunce@bham.ac.uk

ϑ These authors contributed equally to this work.

## Introduction

Acute myeloid leukaemia (AML) is a devastating cancer characterised by the uncontrolled proliferation, abnormal survival and arrested maturation of leukaemic cells within the bone marrow. The rapid expansion of the leukaemic clone reduces haemopoiesis with loss of normal functioning neutrophils, platelets, and erythrocytes. If untreated, most patients die from infection, bleeding and/or anaemia within weeks of diagnosis.

Current best treatments utilise anthracyclines e.g. daunorubicin or idarubicin, alongside the pyrimidine and purine analogue cytarabine with or without 6-thioguanine [1,2]. These drugs non-selectively inhibit DNA and RNA synthesis and consequently their anti-leukaemic activity is associated with high levels of systemic toxicity, including further reduction of haemopoiesis. Although the current therapies of choice, these agents fail to cure more than two thirds of those patients deemed able to tolerate the therapy [2,3,4]. The problem is further exacerbated by the molecular heterogeneity underlying the disease as well as its distribution within the population. AML incidence increases with age and >75% of patients are older than 60 years of age at diagnosis. These older patients have a much reduced capacity to tolerate high dose chemotherapy and their leukaemia's are associated with higher frequencies of unfavourable prognostic factors [5]. As a result,

overall survival rates amongst this cohort are dismal with little improvement having been made over the last 20 years [2,3,4,6,7]. This lack of progress coupled with the frail nature of these patients presents them and their clinicians with limited therapeutic options. The majority of elderly patients receive supportive care alone or with non-intensive therapy [4,8]. A review of 36 AML studies involving a total of 12,370 patients (median age 70 yrs) found that the median overall survival for patients receiving supportive care alone was only 7.5 weeks and for those receiving supportive care with non-intensive therapy only 12 weeks [5].

Knowledge of the molecular pathogenesis of AML and other leukaemia's has led to attempts to develop specific targeted agents and a number of these are now in clinical trial [2,4,9]. However, with the notable exception of all-trans retinoic acid (ATRA) in a subset of AML known as acute promyelocytic leukaemia (APL)[10], and imatinib mesylate (Glivec) and its derivatives in chronic myeloid leukaemia (CML)[11], few of these therapies have as yet had a large scale impact. This has lead to trials using combinations of targeted therapies [12]. However, the problem of developing targeted therapies for AML is complicated by the inherent heterogeneity and genetic complexity of the disease. Thus whilst attempts at new drug discovery remain important, their low success rates, long time scales and high costs impose serious limitations on progress for improving the outlook in this disease.

'Drug redeployment' provides an alternative treatment strategy that is gaining momentum across a broad spectrum of diseases [13,14]. This approach tests the potential of established drugs in new disease settings. We and others have previously demonstrated the individual *in vitro* anti-proliferative and pro-differentiative actions of the sex steroid medroxyprogesterone acetate (MPA) and lipid regulating fibrate drugs against AML cell lines [15,16,17,18], Burkitts lymphoma (BL) cells [19] and chronic lymphocytic leukaemia (CLL) cells [20]. Here we demonstrate improved combinatorial activity of bezafibrate (BEZ) and MPA (B/M) against AML cell lines and primary AML cells. We demonstrate that the activity of the drugs when combined remains selective against AML cells over normal myeloid blasts. Furthermore we demonstrate that the antitumor activity of B/M against AML cell differs from the activity of the same drugs against CLL cells in that it converges on the increased synthesis and decreased metabolism of prostaglandin D$_2$ (PGD$_2$) and its potently anti neoplastic derivative 15deoxy$\Delta^{12,14}$ prostaglandin J$_2$ (15d-PGJ$_2$).Several studies have identified potent activities of 15d-PGJ$_2$ against diverse cancers [21,22,23,24,25,26,27,28,29]. The cyclopentenone configuration of this prostaglandin renders it highly reactive facilitating non-enzymatic covalent bonding to thiol residues in multiple biological substrates [30,31,32,33,34,35,36,37,38]. The result is modulation of the activity and/or levels of multiple cellular targets, the spectrum of which will be cell context specific but which most likely explain the broad anti tumour activity of 15d-PGJ$_2$. Given its bioactive nature, administration of 15d-PGJ$_2$ is likely to be associated with high toxicity and low bioavailability due to conjugation of 15d-PGJ$_2$ to extracellular targets, including serum proteins [39]. An improved strategy is therefore to promote the accumulation of endogenously formed 15d-PGJ$_2$ within target cells. Since 15d-PGJ$_2$ arises non-enzymatically from PGD$_2$ [40,41] the elevated synthesis of this prostanoid is in turn dependent on the elevation of PGD$_2$. We demonstrate here that in the case of AML, elevation of PGD$_2$ and 15d-PGJ$_2$ with associated anti-leukaemic activity can be achieved with drugs that are available, relatively cheap and familiar in the clinical setting.

## Results

### The Anti-Leukaemic Actions of BEZ and MPA against AML Cell Lines Are Most Potent When Combined

Figure 1A shows the dose dependent killing of KG1a cells by MPA and BEZ and illustrates the greater individual potency of BEZ. After 10 days treatment with 0.5 mM BEZ cell viability had been reduced to 20% of controls whereas 5 μM MPA had reduced cell viability to just 60% of controls. In BEZ and MPA cross titration experiments, potentiation of killing of KG1a cells was clearly evident with near total loss of viability with 0.5 mM BEZ and 5 μM MPA after 10 days (Figure 1B). Similar results were also observed in HL60 and K562 cells (data not shown) and are consistent with our previous studies in Burkitt's lymphoma cells [19]. Consequently, all subsequent experiments were performed with 0.5 mM BEZ and 5 μM MPA both when alone and in combination (B/M). The anti-proliferative effects of BEZ and MPA on a panel of cell lines representing diverse forms of AML including U937, NB4 (PML:RAR$\alpha^{+ve}$ APL), HL-60, K562 (BCR:ABL$^{+ve}$ AML blast crisis of chronic myeloid leukaemia) and KG1a cells are shown in Figure 1C and Figure S1. As in KG1a cells, BEZ was the more potent antiproliferative individual agent in U937, NB4 and HL60 cells although neither agent alone was particularly effective against K562 cells. However, B/M treatment was the most potent ($p<0.01$) at reducing cell number across all the cell lines examined.

### BEZ and MPA Variably Induces Differentiation and Apoptosis in Myeloid Cell Lines

The myeloid cell surface antigen CD11b was used in flow cytometry to assess differentiation of U937, NB4, HL60 and KG1a cells. Erythroid differentiation of K562 cells was measured by glycophorin A (Gly A) expression. Consistent with our earlier findings in HL60 cells, MPA alone caused little or no differentiation in any of the cell lines (Figure 2A & Figure S2A) whereas BEZ induced differentiation of U937, NB4 and HL60 cells to varying degrees. Combined B/M treatment induced markedly increased CD11b expression in HL60 cells compared to the individual agents. The combinatorial action of B/M upon HL60 differentiation was confirmed by the reciprocal loss of the more primitive cell marker CD71 (Figure 2B). B/M combined treatment also induced differentiation of U937 and NB4 cells but in these cells there was no increase in B/M over BEZ alone (Figure 2A & Figure S2A). In marked contrast MPA, BEZ and B/M failed to induce either the erythroid or myeloid differentiation of K562 or KG1a cells respectively. This was confirmed by analyses of cell morphology. As shown in Figure 2C, B/M treated NB4 and HL60 cultures clearly contained maturing neutrophils whereas maturing cells were not evident in B/M treated KG1a cultures.

Cell cycle analyses at day 7 identified a marked G1 cell cycle arrest in those cell lines that displayed differentiation in response to B/M (data not shown). In K562, KG1a and U937 but not HL-60 and NB4 cells, cell cycle analyses further identified the accumulation of a sub-G1 fraction, indicative of post apoptotic cells (Figure 2D & Figure S2B). These data indicated that the cell responses to B/M treatment were varied, ranging from strong cell cycle arrest and differentiation to apoptosis. A more detailed comparison of KG1a and HL60 cells confirmed induction of annexin-V labelling (Figure 2E) together with uptake of propidium iodide (PI), consistent with apoptosis in KG1a cells but not in HL60 cells (Figure 2E and 2F).

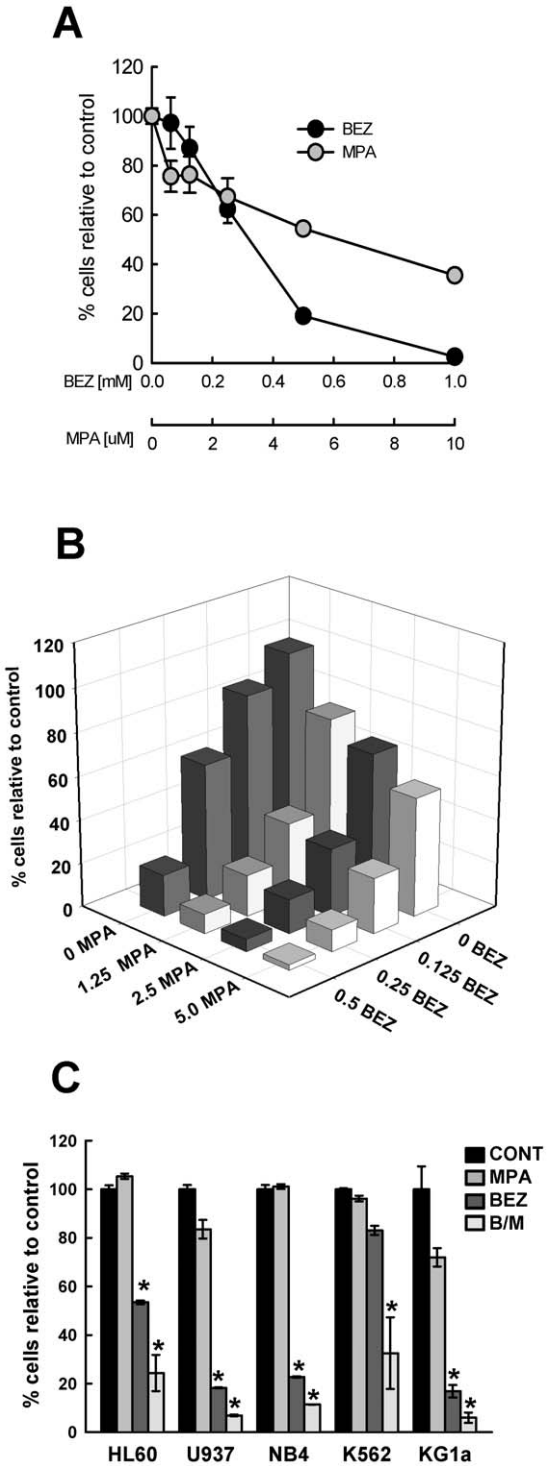


**Figure 1. Dose dependent killing by BEZ, MPA and B/M of myeloid cell lines.** Cell viability as % of solvent treated controls was determined in KG1a cells by Cell-Titre Blue assay following 10 days treatment with (**A**) increasing doses of MPA or BEZ alone, or (**B**) cross-titrations of BEZ (mM) and MPA (μM). Data shown is mean of N = 3 experiments (**C**) 5 different myeloid cell lines were treated with either solvent control, 0.5 mM BEZ, 5 μM MPA or the combination (B/M) for 7 days. Cell viability was calculated for treatments relative to solvent treated controls after readings had been adjusted for feeding regimens over the 7 days of treatment. Mean±sem is shown for 5 cell lines from a minimum of N = 3 experiments. Individual datapoints are shown in Figure S1. Statistics * $p<0.01$.
doi:10.1371/journal.pone.0008147.g001

## In Vitro Anti-Leukaemic Activities of BEZ and MPA Are Recapitulated in Primary AML Cells but Not Normal CD34$^{+ve}$ Cells

Primary AML cells also demonstrated *in vitro* sensitivity to BEZ, MPA and B/M (Figure 3A). At day 8, control cultures originally plated at $1\times10^6$ cells/ml contained $1.1\pm0.13\times10^6$ cells/ml. In contrast B/M treated cultures contained $0.52\pm0.11\times10^6$ cells/ml ($p<0001$). Morphological examination of primary AML cultures (not shown) and cytospins (Figure 3B) prepared from B/M treated AML cells indicated that B/M induced loss of cells was most frequently mediated by cell killing rather than overt differentiation.

In marked contrast, treatment with BEZ, MPA or B/M had little effect on normal myeloid progenitors (CD34+ve cells). Unsorted mobilised mononuclear cells which are enriched with CD34+ve myeloid progenitors were treated for 8 days. No changes in cell number were recorded in response to either drug alone and only a small decrease was observed following B/M treatment. Despite this decrease, the proportion of viable CD34+ve cells increased, indicating no significant loss of these cells (Figure 3C). Similarly, treatment of purified mobilised normal donor CD34+ve cells with BEZ, MPA and B/M did not result in apoptosis or frank differentiation. After 8 days, B/M treated cultures contained 89% of the number of viable cells in untreated cultures. Furthermore, although a slight diminution of CD34 fluorescence intensity was observed, overt differentiation as measured by the maturation marker CD11b was not induced (Figure 3D).

## MPA Targets AKR1C3 in AML Cells

We and others have shown AML cells to express the aldo-keto reductase AKR1C3 [42,43,44] and our rationale for selecting MPA for redeployment as a potential antileukaemic drug is as an inhibitor of this enzyme [28]. However, although MPA had been shown to inhibit other aldo-keto reductases [45], it had not been directly demonstrated as an inhibitor of AKR1C3. Like other members of the AKR1C subfamily of aldo-keto reductases, AKR1C3 displays substrate promiscuity [46] but amongst the human sub-family possesses unique PGD$_2$-11-ketoreductase activity generating 11β-PGF$_{2\alpha}$ from PGD$_2$. Our previous studies have shown that this activity is prominent in AML cells but not detectable in CLL cells [44,20]. MPA inhibited both the cellular AKR1C3 activity in KG1a myeloid cells, as measured by the decreased conversion of $^3$H-PGD$_2$ to $^3$H-11β-PGF$_{2\alpha}$ (Figure 4A), and the *in vitro* activity of recombinant-AKR1C3 protein ($IC_{50}$ = 1.1 μM; Figure 4B). In dose response experiments performed in KG1a cells, the inhibition of AKR1C3 mediated PGD$_2$ conversion to 11β-PGF$_{2\alpha}$ mirrored the dose response of reduced cell viability (Figure 4C). Together these data and those from our previous study that identify AKR1C3 as having PGD$_2$-11-keto reductase activity in AML cell lines [44] support our model of the action of MPA against AML cells.

## The Anti-Leukaemic Activities of BEZ Are Associated with ROS Generation

The original rationale made by ourselves and others for the redeployment of fibrates as anti-AML agents, was based on their activity as ligands for the nuclear receptor PPARα. However, the required BEZ concentrations observed here suggest an alternative mechanism. BEZ has previously been shown to induce oxidative stress in cells [47,48]. In keeping with this, BEZ treatment of K562 and KG1a cells induced a rapid (within 2 hours, data not shown) and sustained generation of reactive oxygen species (ROS) that was BEZ

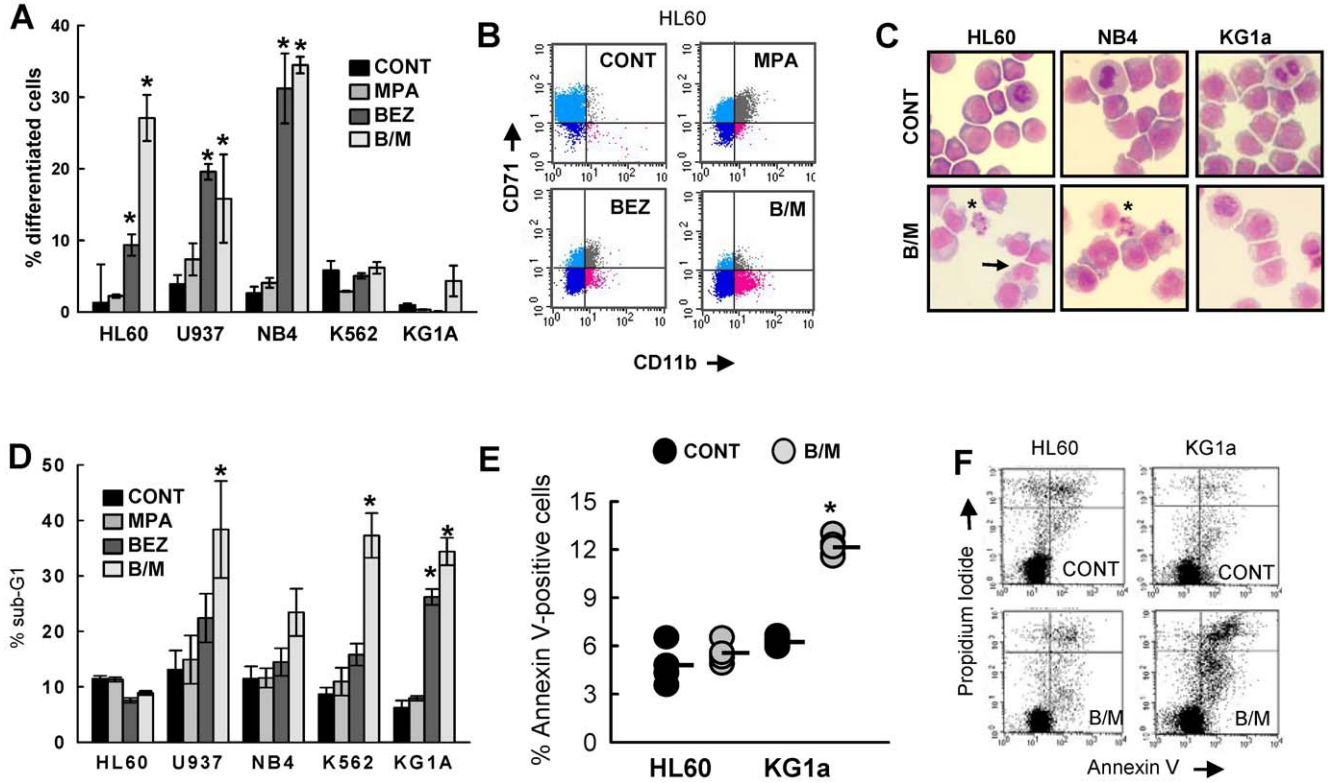


**Figure 2. Cellular consequences of MPA and BEZ treatment.** (**A**) Differentiation was measured by flow-cytometry using the myeloid differentiation antigen CD11b for HL60, NB4, U937, KG1a cells and the erythroid antigen Glycophorin-A for differentiation of K562. Mean data±sem from a minimum of N = 3 experiments are shown. All datapoints are shown in Figure S2A. (**B**) Representative dotplots for HL60 cells following 7 days treatment stained both with CD11b and the proliferation marker CD71. Pale blue shows non-differentiated cells (CD71+, CD11b−), dark blue cells that have lost CD71 (CD71−, CD11b−), and pink identifies differentiated neutrophils (CD71−, CD11b+). (**C**) Cell morphology was analysed by Jenner-Giemsa staining of cytospin preparations of cells treated for 7 days. Apoptotic cells are highlighted by a star and differentiating neutrophils by an arrow. (**D**) % Sub-G1 events were measured by cell cycle analysis of propidium iodide stained cells following 7 days treatment. Mean data±sem for 5 cell lines from a minimum of N = 3 experiments are shown. All datapoints are shown in Figure S2B. (**E**) HL60 and KG1a cells were treated with either solvent CONT or B/M for 48 hours. Apoptosis was assessed by incubation with annexin-V and propidium iodide followed by flow cytometry. Individual datapoints from a minimum of N = 4 are shown with a black bar indicating the mean. (**F**) Representative dotplots of annexin V and propidium iodide stained HL60 and KG1a cells following treatment with either solvent CONT or B/M for 48 hours. Statistics *p<0.01.
doi:10.1371/journal.pone.0008147.g002

concentration dependent (Figure 5A and 5B). Similar induction of ROS was observed in all AML cell lines when treated with 0.5 mM BEZ (Figure 5C). Finally, using the example of KG1a cells, we observed that cell killing by BEZ tightly correlated with the percentage of ROS positive cells (Figure 5D).

## The Actions of BEZ and MPA on AML Cells Converge on the Accumulation of PGD$_2$ and Its Downstream Reactive Product 15d-PGJ$_2$

PGD2 is synthesised from arachidonic acid by both a cyclooxygenase (COX)-dependent pathway [49] and COX-independent, an oxidative stress-dependent, lipid peroxidation-isoprostane pathway [50] (Figure S3). Given that the lipid peroxidation-dependent isoprostane pathway has been shown to be elevated in periods of oxidative stress [51], we postulated that BEZ-induced oxidative stress would result in lipid peroxidation. Consistent with this, 0.5 mM BEZ treatment of AML cell lines labelled with the naturally fluorescent lipid cis-parinaric acid was associated with a significant decrease in fluorescence, indicative of increased lipid peroxidation (Figure 6A). We therefore reasoned that the effects of BEZ and MPA may converge on the elevation of cellular PGD$_2$ via increased lipid peroxidation-mediated synthesis and decreased metabolism by AKR1C3. We also reasoned that as a consequence of increased PGD$_2$ levels, the levels of its potently anti-neoplastic dehydration product 15d-PGJ$_2$ would also be elevated. Indeed, treatment with MPA or BEZ alone and B/M resulted in increased levels of both PGD$_2$ and 15d-PGJ$_2$ in HL60 and KG1a cells (Figure 6B & C). MPA induced 3.3±0.9 fold and 3.8±0.9 fold increases in PGD$_2$ in HL60 and KG1a, respectively as compared to solvent treated control cells (Figure 6B). As may be expected of an inducer of lipid peroxidation and therefore increased isoprostane pathway activity, the effects of BEZ were greater than MPA with 13.7±1.6 and 28.4±9.9 fold increases in PGD$_2$ in HL60 and KG1a, respectively (Figure 6B). B/M gave the most marked elevation especially in HL-60 cells with a 43.4±9.9 fold increase, whereas KG1a had a 35.1±12.2 fold increase. 15d-PGJ$_2$ levels followed a similar trend in both cell lines (Figure 6C).

It has been demonstrated that 15d-PGJ$_2$ itself can potently induce ROS [21]. Consistent with this, treatment of AML cell lines and primary AML cells with 15d$^{-}$PGJ$_2$ also resulted in the induction of ROS levels similar to those seen in response to B/M (Figure S4). Furthermore, treatment of HL60, K562 and KG1a cells with 15d-PGJ$_2$ recapitulated the antiproliferative actions of B/M (Figure 6E) and the enhanced differentiation of HL-60 cells but not of K562 or KG1a cells (Figure 6F).

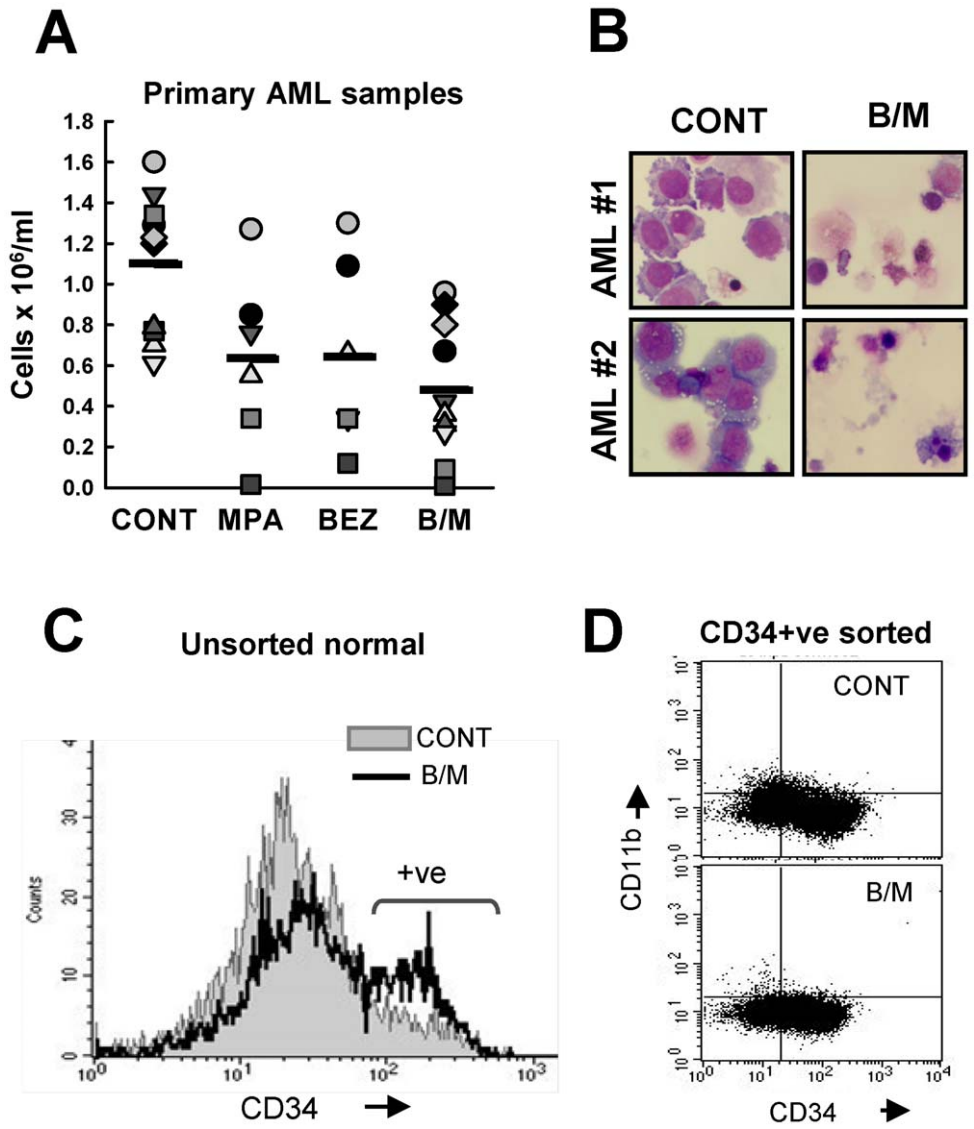


**Figure 3. BEZ and MPA also kill primary AML cells but not normal myeloid progenitors.** (**A**) Primary AML cells were treated for 5 days. Cell numbers were determined by manual counts and are presented as number of cells$\times 10^6$/ml at day 5. The plot shows summary data for 9 individual AMLs and the mean identified by bars. (**B**) Cell morphology for 2 representative AML samples are shown as determined by Jenner-Giemsa staining of cytospin slides. (**C**) Non-sorted mobilised peripheral blood cells were treated with solvent CONT or B/M. Histogram shows representative CD34 staining after 8 days treatment. (**D**) CD34+ve purified normal mobilised cells were treated with either solvent CONT or B/M for 8 days. The dotplots shown are CD34 and CD11b expression following treatment.
doi:10.1371/journal.pone.0008147.g003

## Actions of BEZ and MPA Recapitulate Known Activities of 15d-PGJ$_2$

The above observations suggested that the activities of B/M against AML cells may be largely mediated by the generation of 15d-PGJ$_2$. Previous studies have identified multiple mechanisms by which 15d-PGJ$_2$ exerts its anti-neoplastic activity. The nature and range of these actions suggests that the detailed effects of 15d-PGJ$_2$ against individual tumours may show cell context specificity. We studied some of the previously reported activities of 15d-PGJ$_2$ in AML cells following treatment with BEZ and MPA.

**Glutathione depletion.** The ratio and amounts of reduced glutathione (GSH) and oxidised glutathione (GSSG) are important in regulating the redox state of a cell. Under conditions of oxidative stress, GSH/GSSG levels become depleted and imbalanced, leading to cell differentiation or cell death. Importantly, 15d-PGJ$_2$ concentrations that induce apoptosis and differentiation have been associated with depletion of cellular GSH [21,52]. Furthermore, 15d-PGJ$_2$ levels have been shown to be tightly regulated through GSH-conjugation and subsequent cellular export [53,54,55]. We therefore determined changes in GSH levels following treatment with BEZ, MPA and B/M. Significant decreases in both GSH (Figure 7A) and GSSG (Figures S5 & S6) levels were observed following drug treatment. In the case of GSH reduction the B/M effect was not greater than either drug alone whereas the greatest reduction in GSSG was observed in response to B/M (Figure S6).

**PPARγ activation.** Amongst the first biological activities ascribed to 15d-PGJ$_2$ was as an activating ligand for the nuclear receptor PPARγ [56,57]. Luciferase reporter assays in transiently transfected HL60 cells identified PPARγ-activation in response to MPA, BEZ and B/M (Figure 7B). Although small, the observed

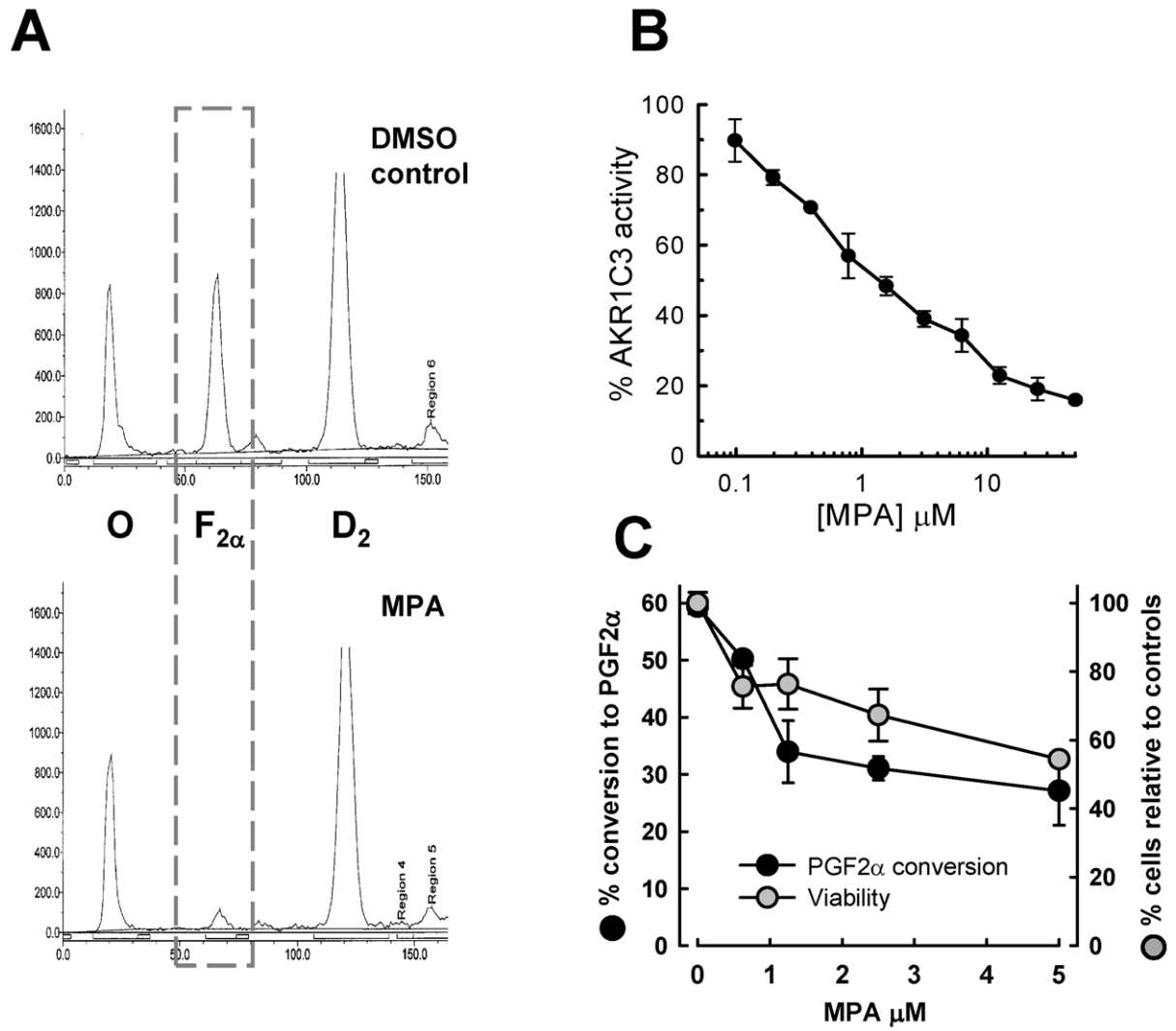


**Figure 4. MPA inhibits AKR1C3 PGD$_2$ 11β keto-reductase activity.** (**A**) $^3$H-PGD$_2$ turnover was determined by thin layer chromatography (TLC) on KG1a cells treated with either solvent control or 5 μM MPA. Representative TLC traces are shown from a minimum of N = 4 experiments. Abbreviations; O = origin, F$_{2\alpha}$ = 11β-PGF$_{2\alpha}$, D$_2$ = PGD$_2$. (**B**) Inhibition of recombinant AKR1C3 protein activity by MPA. The plot shows percentage of AKR1C3 activity in the presence of increasing concentrations of MPA relative to AKR1C3 in the absence of MPA. The data are means±s.d. from a single experiment performed in triplicates. (**C**) Conversion of $^3$H-PGD$_2$ to 9α-11β-PGF2α was determined by TLC in KG1a cells treated with MPA titrations and compared to cell viability at day 10. Mean data±sem from a minimum of N = 3 are shown.
doi:10.1371/journal.pone.0008147.g004

changes in PPARγ-activation mirrored those seen with 5 μM 15d-PGJ2 treatments.

**IκB-accumulation.** 15d-PGJ$_2$ has been shown to regulate NF-κB activity at multiple levels [30,31]. This includes regulation of IκB (inhibitor of κB) protein levels by inhibiting the activity of the IKK (Iκ*B*-kinase) complex that targets IκB for ubiquitin-mediated protein degradation [30]. Inhibition of IκB-phosphorylation results in its accumulation and consequent inhibition of NF-κB transcriptional activity. Western blot analysis revealed IκB-accumulation in MPA, BEZ and B/M treated HL60 cells (Figure 7C & D, Figure S7). The pattern of IκB accumulation mirrored that of 15d-PGJ$_2$ accumulation with MPA having the least or little effect, BEZ having a greater effect and the combination being most effective. Similar accumulations were observed in U937 cells and in a sample of primary AML cells, (Figure 7D) however KG1a and NB4 cells did not show an accumulation of IκB (Figure 7C&D, Figure S7). Since 15d-PGJ$_2$ is known to regulate NF-κB transcriptional activity at multiple levels we cannot rule out the possibility that B/M may alter NF-κB in KG1a and NB4 cells by mechanisms other than accumulation of IκB.

## The Cellular Activities of BEZ and MPA Are Enhanced by Physiological Levels of Vitamin A and Vitamin D$_3$

When considering the translation of this study into a clinical trial we wished to better understand how to exploit these effects. Since we and others have previously shown that fibrates and MPA each separately enhance ATRA and 1α,25(OH)$_2$ vitamin D$_3$ (D3) induced HL-60 cell differentiation [15,17,58] we reasoned that where the combined action of B/M results in differentiation this may be reciprocally limited in the absence of ATRA and D3. In an attempt to mimic physiological levels of ATRA and D$_3$ that might be expected in patients with adequate daily vitamin A and D intake, we treated HL60 cells with B/M together with 1 nM ATRA, 1 nM D$_3$ and the combination (ATRA/D$_3$). As in

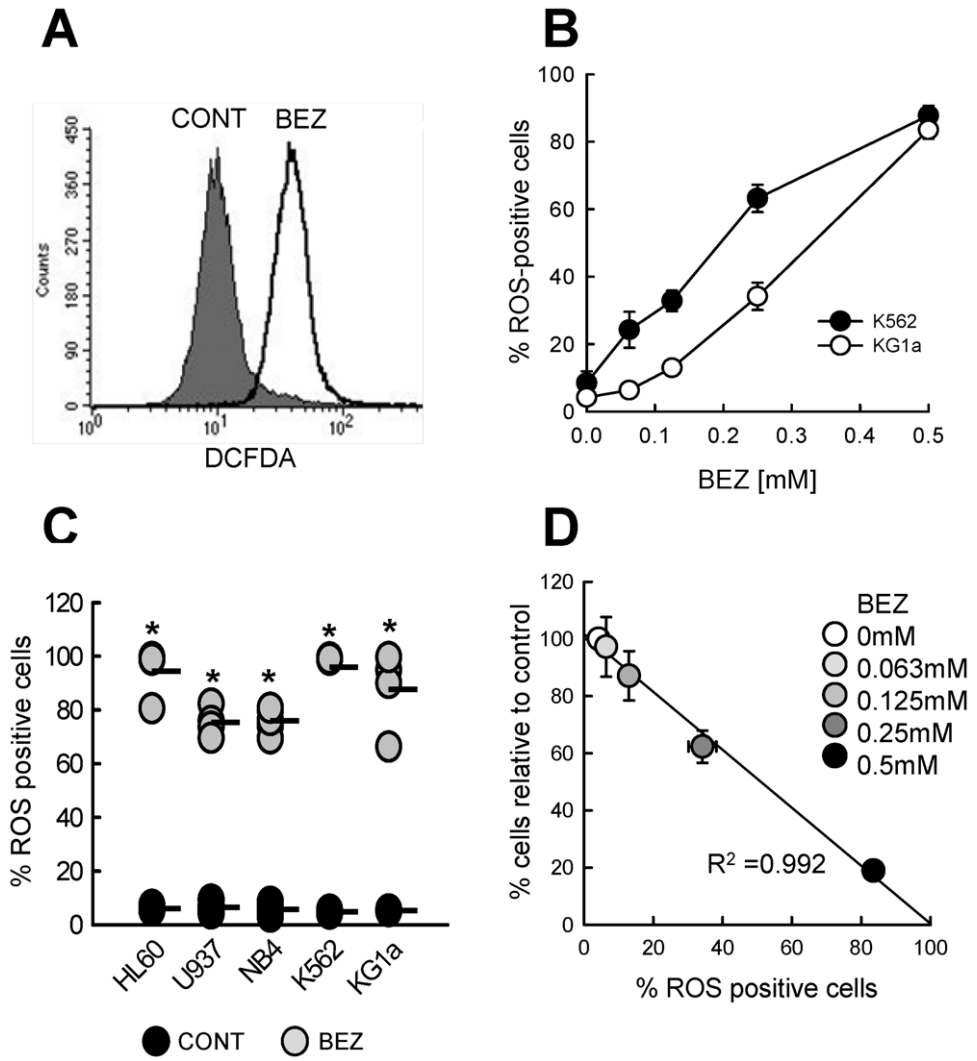


**Figure 5. BEZ induction of ROS is concentration dependent and correlates with cell killing.** BEZ induced reactive oxygen species (ROS) were measured at 14 hours by staining with carboxy-$H_2$DCFDA and analysis by flow cytometry. (**A**) Histogram shows representative results from HL60 cells. (**B**) ROS induction was measured in K562 and KG1a cells after 14 hrs treatment with different BEZ concentrations (mean±sem from N = 4 experiments). (**C**) ROS induction with 0.5 mM BEZ for 5 myeloid cell lines is shown from a minimum of N = 3 experiments for each cell line. Mean is indicated by black bar. (**D**) % viable KG1a cells at day 10 compared to controls plotted against the % cells positive for ROS at increasing BEZ concentrations. Statistics *$p<0.01$.
doi:10.1371/journal.pone.0008147.g005

Figure 2A, B/M alone caused differentiation in ~20% of HL60 cells, 1 nM ATRA+1 nM $D_3$ (ATRA/$D_3$) alone caused differentiation in ~35% as measured by expression of the differentiation marker CD11b at day 7 (Figure 8A). However, morphologically relatively few cells had reached terminal neutrophil differentiation (Figure 8B). Addition of ATRA or D3 individually to B/M resulted in a significant increase in differentiated cells (Figure 8A). However, the addition of B/M together with ATRA/$D_3$ resulted in ~90% of cells expressing increased CD11b and morphologically all cells had differentiated into polymorphonuclear neutrophils and/or undergone apoptosis (Figure 8A & B) demonstrating strong complementary interactions between B/M and physiological levels of ATRA and $D_3$. Prolonged survival and differentiation was rarely seen in primary AML cells however, when it did occur, we also observed complimentarity between B/M and ATRA/D3. This is illustrated in the primary AML (non-APL) sample shown in Figure 8C. CD11b expression was detected in 4.5% of control cells compared to 17.5% in ATRA/D3 treated cells. B/M alone induced CD11b expression in 32%, which was further increased to 46% when cells were treated with B/M & ATRA/D3 (Figure 8C). Interestingly, the addition of ATRA/D3 did not interfere with induction of ROS by B/M indicating that these agents were working by complementary actions (Figure 8D).

## Discussion

Drug redeployment has already demonstrated great promise in haemato-lymphoid malignancies including, thalidomide in myeloma [59] and valproic acid and arsenic trioxide in AML [60,61]. However, few studies have sought to redeploy combinations of old drugs that deliver greater potency than either drug alone. We demonstrate here that exploiting some understanding of the mechanisms of drug actions against cancer cells allows the rational testing of such potentially beneficial combinations.

The anti-neoplastic activities of 15d-PGJ$_2$ have been described in many reports [21–29], however few studies have sought

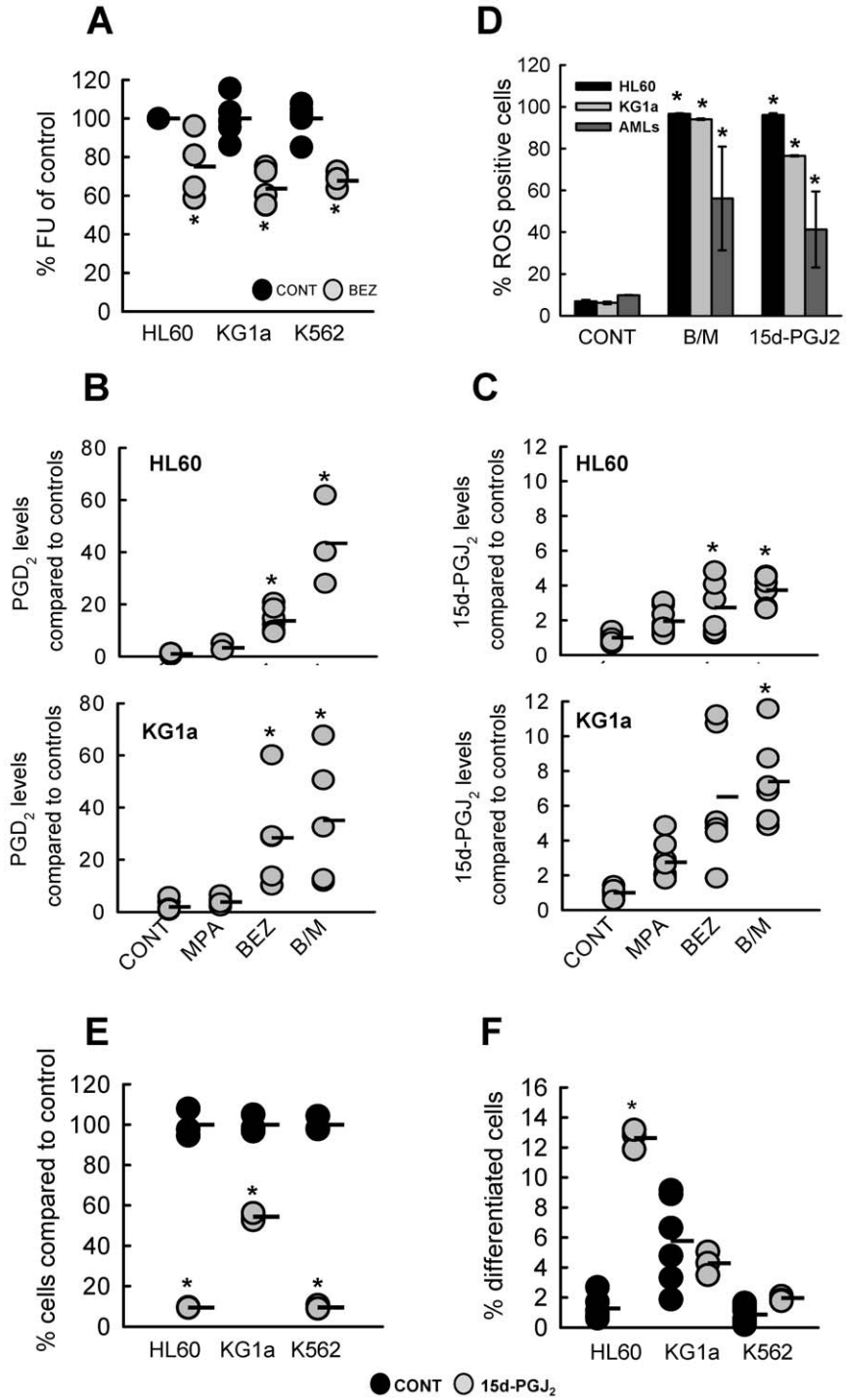


**Figure 6. BEZ and MPA modulate PGD$_2$ and 15d-PGJ$_2$ levels.** (**A**) 0.5 mM BEZ induced lipid peroxidation was measured by treating cells labelled with the naturally fluorescent lipid *cis*-parinaric acid. Data is presented as % fluorescence units (FU) compared to solvent control cells for N = 5 experiments for each cell line. Mean is indicated by black bar. (**B & C**) Endogenous levels of (**B**) PGD$_2$ and (**C**) 15d-PGJ$_2$ were determined in HL60 and KG1a cells by ELISA following 2 hours treatment. Prostaglandin levels are shown relative to untreated controls for a minimum of 4 experiments. Mean is indicated by black bars. Statistics: * $p<0.05$. (**D**) ROS induction was determined by staining with DCFDA and flow cytometry in HL60, KG1a and primary AML samples (n = 3) after 48 hours treatment with CONT, B/M or 10 μM 15d-PGJ$_2$. Data shown are mean±sem. Individual datapoints are shown in Figure S4. (**E & F**) HL60, K562 and KG1a cells were treated for 7 days with either solvent control or 5 μM 15d-PGJ$_2$. Data is shown from a minimum of N = 3 experiments. Mean is indicated by black bar. (**E**) Cell viability was assessed by Alamar blue and calculated as % of control cells. (**F**) Differentiation was assessed by CD11b staining of HL60 and KG1a and GlyA staining of K562 cells followed by flow cytometry. Statistics: * $p<0.01$.
doi:10.1371/journal.pone.0008147.g006

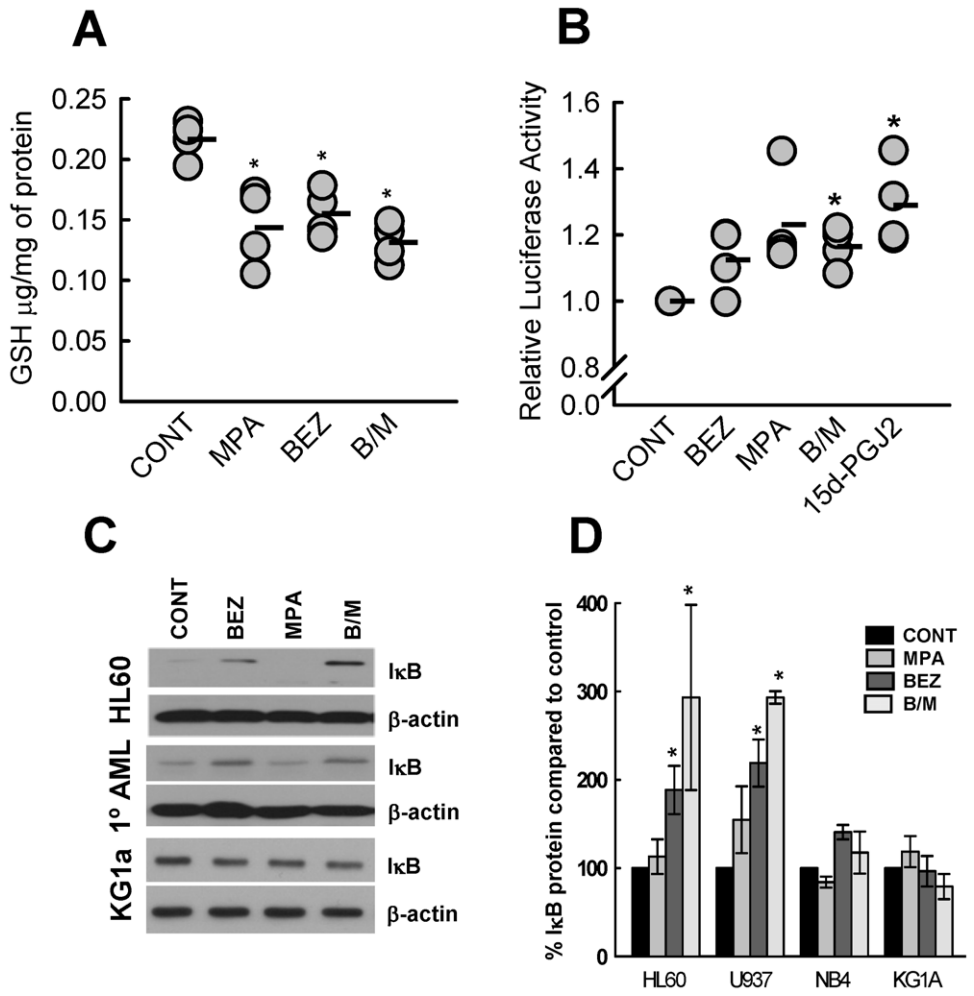


**Figure 7. Downstream consequences of elevating 15d-PGJ$_2$ levels.** (**A**) Elevating 15d-PGJ$_2$ levels results in lowering of reduced-glutathione (GSH). HL60 cells were treated for 48 hours and µg GSH per mg of protein measured. Data shown is from 4 experiments and the mean is indicated by a black bar. (**B**) PPARγ transcriptional activity was measured after 14 hours treatment of PPRE-luciferase reporter plasmid and pRenilla luciferase transfected HL60 cells with either MPA, BEZ, the combination (B/M) or 5 µM 15d-PGJ$_2$ (PGJ$_2$). Data shown is luciferase activity compared to control untreated cells for N = 5 experiments. Mean is indicated by black bar. (**C&D**) IκB levels were determined by western blotting of cells treated for 14 hrs. Levels were normalised for loading by β-actin westerns. (**C**) Representative western blot results for HL60, KG1a and a primary AML. (**D**) Graph represents mean±sem of densitometry performed on a minimum of N = 3 experiments for each cell line. All individual datapoints are shown in Figure S7. Statistics: * $p<0.05$.
doi:10.1371/journal.pone.0008147.g007

strategies for utilising this potential. Although a novel cycloanthanilylproline derivative, Fuligocandin B, has been shown to induce 15d-PGJ$_2$ production in treated cells the compound has yet to undergo toxicity testing in humans [62]. Here, we demonstrate that 15d-PGJ$_2$ and its precursor, PGD$_2$, can be elevated in AML cells using already available drugs with good safety profiles. BEZ treatment mediated sustained ROS generation with associated lipid peroxidation, downstream synthesis of PGD$_2$ and consequently, generation of 15d-PGJ$_2$. MPA, further elevated PGD$_2$ and 15d-PGJ$_2$ levels by inhibiting the metabolism of PGD$_2$ by AKR1C3 (Figure S8).

15d-PGJ$_2$ is a cyclopentenone prostaglandin. These prostaglandins have unsaturated α,β ketone moieties that allow non-enzymatic covalent modification of cellular targets [63]. It is this reactive nature that is thought to be responsible for their potent and wide-ranging properties [63,64]. Proteomic approaches have identified the conjugation of 15d-PGJ$_2$ with many protein targets including multiple components of mitochondria, the cytoskeleton and also transcriptional networks such as NF-κB [30–38]. Importantly, B/M treatment of AML cell lines and primary AMLs recapitulated some of the known anti-neoplastic activities of 15d-PGJ$_2$. However these actions were not uniform across all the cell types tested. Similarly, we observed differential apoptotic and differentiation responses to B/M in both AML cell lines and primary AML cells. These variations may reflect the molecular heterogeneity of AML and the consequent contextual actions of 15d-PGJ$_2$.

In contrast, 15d-PGJ$_2$ also generated ROS in all AML cell lines and primary AML cells tested. It may therefore be that B/M treatment induces a cycle of direct and secondary 15d-PGJ$_2$-mediated ROS generation thereby perpetuating a cycle of glutathione depletion and oxidative stress. The importance of ROS as well as 15d-PGJ$_2$ in mediating the anti-leukaemic activity of B/M is highlighted by our recent NMR based metabolomics study of B/M treated AML cell lines [18]. It has been shown that ROS mediates the direct chemical conversion of α-ketoglutarate to succinate [65,66,67]. Notably, our metabolomics study identified

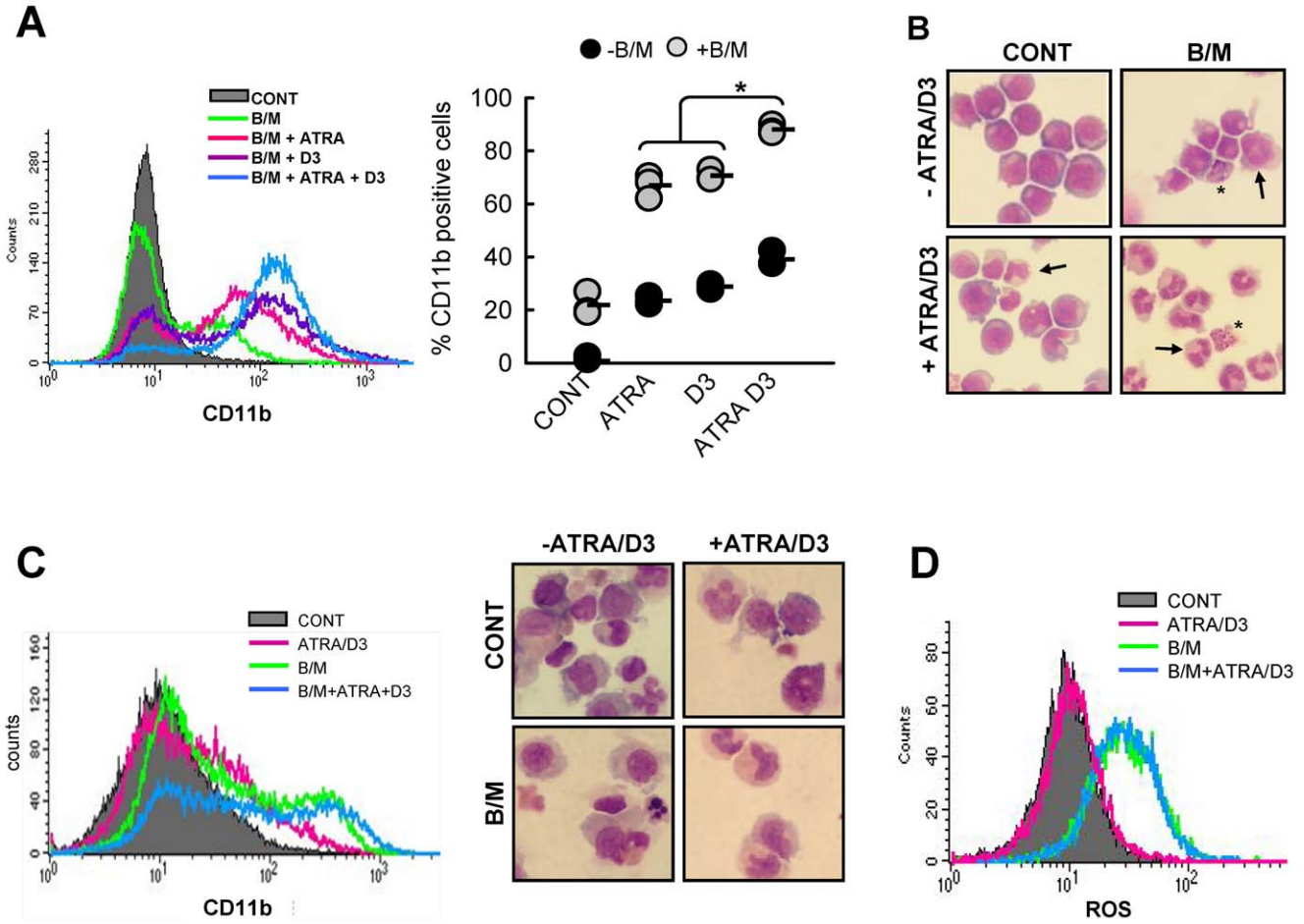


**Figure 8. Physiological levels of ATRA and Vitamin D3 potentiate the actions of BEZ and MPA.** (**A**) HL60 cells were treated for 7 days with solvent control, B/M alone and B/M combined with either 1 nM ATRA, 1 nM 1α,25(OH)$_2$ vitamin D$_3$ (D$_3$) or both. A representative histogram of CD11b flow cytometry is shown in the *left panel* and results from N = 4 experiments in the *middle panel*. Mean is indicated by the black bar. (**B**) Cell morphology was analysed by Jenner-Giemsa staining of cytospins. Differentiated neutrophils are identified by classical poly-lobed nuclei (arrows) and apoptotic cells highlighted by asterix. Statistics: *$p<0.001$. (**C**) Primary AML cells taken from a karyotypically normal non-APL AML were treated with solvent CONT, B/M±1nmATRA/1nM D3. Differentiation was determined by CD11b staining and flow cytometry and by morphological analysis of Jenner-Giemsa stained cytospins after 18 days of treatment. (**D**) ROS generation was measured as described above in primary AML cells treated with cont, B/M±1nmATRA/1nM D3 for 48 hours.
doi:10.1371/journal.pone.0008147.g008

drug mediated imbalances within the TCA cycle including the depletion of α-ketoglutarate and the accumulation of succinate [18]. This effect was recapitulated in cell extracts by the application of the ROS hydrogen peroxide. Therefore the antileukaemic actions of B/M against AML are complex and most likely mediated by separate and overlapping actions of both 15d-PGJ$_2$ and ROS.

Although our studies have focused upon the accumulation of PGD$_2$ and 15d-PGJ$_2$ in B/M treated AML cells, it should not be ignored that part of the activity of MPA against AML cells may also be mediated by the diminution of 11β-PGF$_{2\alpha}$ (Figure S8) and future studies should address this possibility. Furthermore, since the anti-neoplastic activities of 15d-PGJ$_2$ have been demonstrated in multiple tumour models [21–29], the potential of B/M based therapy may also extend beyond AML into other 15d-PGJ$_2$ sensitive tumours. Our observations that B/M has greater efficacy against CLL, BL and now AML cells than either BEZ or MPA alone would appear to support this contention. However, it is important to note that although we have demonstrated that CLL cells express AKR1C3 we were unable to demonstrate AKR1C3 PGD$_2$-11-ketoreductase activity in these cells [20]. These observations indicate that the substrate promiscuity of AKR1C3 is of real biological importance and has implications for its functions in different cell contexts. Hence, further studies are required to determine how B/M and particularly MPA or other AKR1C3 inhibitors exert anti tumour activities in different tumour settings.

In summary our findings support the investigation of B/M as novel therapy in elderly and relapsed AML. We have instigated such a trial, the results of which will be published in the near future. Given the low direct and supportive care costs of these agents, and their activity against multiple tumour types this study identifies an affordable potential anti-cancer therapy in developing countries where fiscal and other restraints limit the availability of conventional chemotherapy.

## Materials and Methods

### Reagents

Bezafibrate (0.5 M in DMSO), MPA (5 mM in ethanol), ATRA (1 mM in DMSO), and 1α, 25(OH)$_2$ vitamin D$_3$ (1 mM in

ethanol) (Sigma Aldrich). PGD$_2$ and 15d$\Delta$-$^{12,14}$PGJ$_2$ (Affiniti, UK) were dissolved in DMSO to yield 20 µM stocks and stored at −20°C.

## In Vitro Recombinant AKR1C3 Activity Assay

Recombinant N-terminal His-tagged recombinant AKR1C3 was produced as previously described [68]. Enzyme reactions (1 ml-volumes) contained 15 µg recombinant AKR1C3, 4 µM phenanthrenequinone (Sigma, UK), 150 µM NADPH (Sigma) and 0–100 µM MPA in 50 mM potassium phosphate buffer (pH 6.5) at 35°C and measured as the rate of change of pyridine nucleotide absorbance at 340 nm.

## Primary Cells, Cell Lines and Treatments

HL-60, NB4, U937, K562 and KG1a myeloid cell lines were maintained in RPMI 1640 medium supplemented with 10% (v/v) heat-inactivated fetal bovine serum (FBS) and penicillin/streptomycin (Gibco, Invitrogen Ltd, UK). Unless specified otherwise, $1\times10^6$ cells in 4 mls were treated with solvent control, 5 µM MPA, 0.5 mM BEZ or the combination B/M. 1 nM ATRA+1 nM Vitamin 1,25(OH)$_2$ vitamin D$_3$ (D3) (Sigma, UK), 10 µM PGD$_2$ or 5–10 µM 15d-PGJ$_2$ were added where specified. Primary AML mononuclear cell preparations were prepared using Ficoll Paque-Plus (Pharmacia Biotech, UK) from presentation aspirates and peripheral blood samples provided after informed consent and ethical committee approval from ongoing phase I/II trials currently undertaken within the University of Birmingham Hospitals NHS Trust and from the MRC AML 15 phase III trial. The resultant AML blast preparations were cultured at $1\times10^6$ cells/ml in RPMI 1640 supplemented with 1% (v/v) ITS$^+$ (VWR, UK), IL3 (1 ng/ml) and SCF (10 ng/ml) (both R&D Systems, UK). For treatments, primary AML cells were set at $1\times10^6$ cells/ml with either solvent control, 5 µM MPA, 0.5 mM (500 µM) BEZ or B/M, ±1 nM ATRA+D3. Viability was determined by manual cell counts and cytospin preparations made for analysis of morphology. Normal donor mobilised peripheral blood samples were provided under ethical approval and informed consent by the National Blood Service, Stem Cell Laboratories, Birmingham, UK, and treated as for primary AML cells.

## $^3$H-PGD$_2$ Turnover Analysis by Thin Layer Chromatography

PGD$_2$ turnover in intact cells was determined similarly to that described previously [28]. Briefly, $2\times10^6$ KG1a cells were incubated with 0.2 µCi/1.3pmoles $^3$H-PGD$_2$ (Amersham Biosciences) in warm PBS for 9 hours. Prostaglandin extracts were prepared from supernatants and separated on silica gel/TLC plates before reading on a Bioscan plate reader. Prostanoids were identified by their co-migration with known standards (Biomol International L.P., UK) visualized by placing in a sealed tank filled with iodine vapor for approximately 5 minutes.

## Lipid Peroxidation Assay

$2\times10^6$ cells at $2.5\times10^5$/ml were treated at 37°C for 2 hours with the addition of 10 µM *cis*-parinaric acid (a naturally fluorescent lipid) for the last 30 mins. Cells were harvested and lipids extracted in the dark for 1 hour with isopropanol + 0.05% butylated hydroxytoluene. Fluorescence readings were taken at 320 nm$_{excitation}$/415 nm$_{emission}$. Background fluorescence of lipids extracted from unlabelled control cells was subtracted from all values and data presented as % fluorescence units (FU) compared to solvent control cells.

## Assessment of Accumulation of ROS

Cells were treated for 14 hours at 37°C and 10 µM carboxy-H$_2$DCFDA (Molecular Probes, Invitrogen, UK) added to cells for the final 45 mins. Following incubation, cells were washed with PBS and analysed by flow cytometry (Becton Dickinson FACS Calibur and Becton Dickinson Cell Quest software).

## Prostaglandin ELISAs

Prostaglandin D2-MOX EIA kit (Cayman Chemicals, USA) and 15$\Delta^{12,14}$Prostaglandin J2 Enzyme Immunoassay Kit (Assay Designs, Inc., USA) were used to determine prostaglandin levels. $5\times10^6$ cells were treated for 2 hours. Following treatment, cells were harvested with 1 ml culture media and homogenised using a Precellys 24 ceramic bead based homogenisation system. Prostaglandins were extracted using C18 reverse phase extraction columns (Chromabond, Fisher, UK) and levels determined by ELISA.

## Measurement of GSH Levels

$3\times10^6$ cells were treated at $2.5\times10^5$/ml, cell pellets prepared and GSH levels determined as described previously [69].

## PPRE Reporter Assays

Briefly, $2\times10^6$ HL-60 cells were transfected with 2.5 µg p4xACO-Luciferase (kind gift from Prof Bert Vogelstein, John Hopkins, USA) and 0.5 µg pRenilla-luciferase (Promega, UK) using Solution V and file T19 on the AMAXA Nucleofector I system. Transfected cells were allowed to recover for 14 hrs and then treated for 24 hrs. Cells were harvested and luciferase measured using the Dual-Glo® Luciferase Assay Kit (Promega, UK) according to manufacturer's instructions.

## Western Blot Analyses

Cells treated with drugs for 14 hrs were lysed in RIPA buffer and 30 µg proteins separated by SDS-PAGE. Proteins were transferred to Immobilon-P membrane (Millipore Corp, Bedford, MA, USA) and probed with 1/1000 dilution of anti-IκB (Santa Cruz, USA). Detection was by anti-rabbit-horse radish peroxidise (HRP) diluted 1/1000 and ECL using Supersignal West Pico Chemiluminescent substrate (Pierce, USA). Loading controls used anti β-actin antibody (Sigma UK) diluted 1/25000 and anti-mouse-HRP secondary at 1/25000. Densitometry was performed using ImageJ software (http://rsb.info.nih.gov/ij/) and IκB protein expression normalised to β-actin.

## Measurement of Relative Number of Viable Cells

Myeloid cell lines were treated for 7 days with refeeding every 2 days. Numbers of viable cells in triplicate 100 µl aliquots of cultures were determined using CellTiter-Blue® reagent (CellTiter-Blue® Cell Viability Assay, Promega, UK). Readings were adjusted for feeding schedules over the course of treatment.

## Assessment of Cell Differentiation

Myeloid cell lines were treated for 7 days with refeeding and retreating every 2 days. Analysis of differentiation antigen expression was by flow cytometry (Becton Dickinson FACS Calibur and Becton Dickinson Cell Quest software) using FITC CD71 and PE-CD11b (Becton Dickinson) conjugated antibodies for HL60, U937, NB4 and KG1a cells. FITC-Glycophorin-A was used to determine erythroid differentiation of K562 (Serotec, UK).

## Assessment of Apoptosis by Annexin-V

Phosphotidylserine cell surface expression was assessed using Annexin-V FITC kit (Becton Dickinson, UK). Analyses were

carried out by Flow cytometry on a Becton Dickinson FACS Calibur utilising Cell Quest Pro software (Becton Dickinson, UK).

### Jenner Giemsa Staining of Slides

Cytospins were prepared from 75–100 µl of culture. Slides were air-dried, methanol fixed and stained; first with Jenner staining solution (VWR, UK) diluted 1/3 in 1 mM sodium phosphate buffer pH 5.6 (5 mins) and second with Giemsa stain (VWR, UK) diluted 1/20 in 1 mM sodium phosphate buffer pH 5.6 (10 mins). Slides were dried and then mounted onto coverslips using DePex (VWR, UK).

### Statistics

Data were analysed using SPSS v15 and the non-parametric Mann-Whitney U test. Unless stated in the legend, the statistics shown in figures are all compared to control cultures.

## Supporting Information

**Figure S1** Cell viability is reduced in Myeloid cell lines treated with BEZ, MPA or B/M. Cell viability as % of solvent treated controls was determined in 5 myeloid cell lines by Alamar Blue assay following treatment with either solvent control, 0.5 mM BEZ, 5 uM MPA or the combination (B/M) for 7 days. Cell viability was calculated for treatments relative to solvent treated controls after readings had been adjusted for feeding regimens over the 7 days of treatment. Mean is indicated by the black bars. Statistics * $p<0.01$.
Found at: doi:10.1371/journal.pone.0008147.s001 (0.12 MB PPT)

**Figure S2** Effect of BEZ, MPA and B/M on myeloid cell lines. (A) Differentiation was measured by flow-cytometry using the myeloid differentiation antigen CD11b for HL60, NB4, U937, KG1a cells and the erythroid antigen Glycophorin-A for differentiation of K562. Scatter plots show data from a minimum of N = 3 experiments. Mean is indicated by black bar. (B) % Sub-G1 events were measured by flow cytometry cell cycle analysis of propidium iodide stained cells following 7 days treatment. Scatter plot shows data from a minimum of N = 3 experiments. Mean is indicated by black bar.
Found at: doi:10.1371/journal.pone.0008147.s002 (0.21 MB PPT)

**Figure S3** PGD$_2$ synthesis, metabolism and non-enzymatic conversions towards 15d$\Delta^{12,14}$PGJ$_2$. Adapted from Gao et al, 2003 (JBC 278: 28479–89). PGD$_2$ is highly unstable and rapidly undergoes non-enzymatic conversions to form 15d$\Delta^{12,14}$PGJ$_2$ in the absence of AKR1C3. Solid arrows and dotted arrows indicate enzyme mediated and non-enzymatic conversions respectively.
Found at: doi:10.1371/journal.pone.0008147.s003 (0.09 MB PPT)

**Figure S4** ROS induction in myeloid cell lines and primary AMLs. Reactive oxygen species (ROS) induction was determined by staining with carboxy-H2 DCFDA and flow cytometry in HL60, KG1a and primary AML samples after 48 hours treatment with CONT, B/M or 10 mM 15d-PGJ2. Data shown is N = 4 for HL60 and KG1a and N = 3 primary AMLs. Mean is indicated by black bar. Statistics * $p<0.01$
Found at: doi:10.1371/journal.pone.0008147.s004 (0.06 MB PPT)

**Figure S5** 1H-1H 2D correlation spectroscopy (COSY) NMR spectrum of KG1a cells extracts. Expanded region (2.6–4.8 ppm) of 1H-1H 2D COSY 45 (COrrelation SpectroscopY) NMR spectrum acquired on dried polar extracts of KG1a cells (solvent control treatment) redissolved in 99.9% D2O (GOSS Scientific Instruments Ltd, Essex UK). 2D COSY experiments were carried out using 800 MHz Varian spectrometer equipped with a cryogenically cooled probe using a gradient-selected coherence transfer pathway (gCOSY45) (Hurd, John & Plant, 1991, J Mag Reson, 93: 666) with 16 transients of 8192 complex data points, 256 increments, and a spectral width of 8 kHz in both dimensions. The highlighted peaks (red lines) are due to oxidized (GSSG) and reduced (GSH) glutathione.
Found at: doi:10.1371/journal.pone.0008147.s005 (0.42 MB PPT)

**Figure S6** 1H 1D NMR spectrum of KG1a cells extracts. Cells were treated for 24 hours and polar extracts analysed by NMR. Extraction of metabolites from cells pellets was performed using a modified Bligh-Dyer procedure. Dried polar extracts were redissolved in 90% $H_2O$/10% $D_2O$ (GOSS Scientific Instruments Ltd, Essex UK) with phosphate buffer (100 mM, pH 7), containing 0.5 mM TMSP. A 500 MHz Bruker spectrometer equipped with a cryogenically cooled probe was used for 1D 1H data acquisition. The water resonance was suppressed using excitation sculpting (Hwang & Shaka, 1998, J Magn Reson, 135: 280). 1D spectra were acquired using a 60° pulse, a 5 kHz spectral width, a relaxation delay of 3 s with 128 transients. 3 different sections (2.15–2.22, 2.50–2.62, and 2.95–3.02 ppm) of the 1H 1D NMR spectrum of KG1a cell extracts containing glutathione peaks. A minimum of 12 replicates for each treatment (black, solvent control; red, MPA, green BEZ, blue B/M) are shown. The insert depicts the average spectrum of 12 replicates expanded between 2.15–2.22 ppm.
Found at: doi:10.1371/journal.pone.0008147.s006 (0.22 MB PPT)

**Figure S7** I-kappa B levels are reduced in some myeloid cell lines following treatment with B/M. IkB levels were determined by western blotting of cells treated with either solvent control, 0.5 mM BEZ, 5 µM MPA or the combination for 14 hrs. Levels were normalised for loading by β-actin westerns and densitometry. Scatter plots show all datapoints for a minimum of N = 3 experiments for each cell lines. Means are indicated by black bars. Statistics *$p<0.05$
Found at: doi:10.1371/journal.pone.0008147.s007 (0.11 MB PPT)

**Figure S8** Model of B/M action against AML cells. ROS directly generated by BEZ and indirectly by subsequently generated 15-deoxy-$\Delta^{12,14}$PGJ$_2$, enhances PGD$_2$ production via the lipid peroxidation isoprostane pathway. Inhibition of AKR1C3 by MPA results in diversion of PGD$_2$ towards the J series prostaglandins culminating in the pleiotropic anti neoplastic actions of 15-deoxy-$\Delta^{12,14}$PGJ$_2$ including further generation of ROS and activation of lipid peroxidation.
Found at: doi:10.1371/journal.pone.0008147.s008 (0.10 MB PPT)

## Author Contributions

Conceived and designed the experiments: FLK JPR MRV UG JCM HS JAM MTD CB. Performed the experiments: FLK REH JB AL ST NJD RMG. Analyzed the data: FLK REH JB AL ST NJD JPR MRV UG JCM RMG MTD CB. Contributed reagents/materials/analysis tools: JPR MRV UG HS MTD CB. Wrote the paper: FLK REH NJD JAM MTD CB.

## References

1. Craig CM, Schiller GJ (2008) Acute myeloid leukemia in the elderly: conventional and novel treatment approaches. Blood Rev 22: 221–234.
2. Estey E (2007) Acute myeloid leukemia and myelodysplastic syndromes in older patients. J Clin Oncol 25: 1908–1915.

3. Kohrt HE, Coutre SE (2008) Optimizing therapy for acute myeloid leukemia. J Natl Compr Canc Netw 6: 1003–1016.
4. Tallman MS, Gilliland DG, Rowe JM (2005) Drug therapy for acute myeloid leukemia. Blood 106: 1154–1163.
5. Deschler B, de Witte T, Mertelsmann R, Lubbert M (2006) Treatment decision-making for older patients with high-risk myelodysplastic syndrome or acute myeloid leukemia: problems and approaches. Haematologica 91: 1513–1522.
6. Burnett AK, Milligan D, Goldstone A, Prentice A, McMullin MF, et al. (2009) The impact of dose escalation and resistance modulation in older patients with acute myeloid leukaemia and high risk myelodysplastic syndrome: the results of the LRF AML14 trial. Br J Haematol 145: 318–332.
7. Burnett AK, Mohite U (2006) Treatment of older patients with acute myeloid leukemia–new agents. Semin Hematol 43: 96–106.
8. Goldstone AH, Burnett AK, Wheatley K, Smith AG, Hutchinson RM, et al. (2001) Attempts to improve treatment outcomes in acute myeloid leukemia (AML) in older patients: the results of the United Kingdom Medical Research Council AML11 trial. Blood 98: 1302–1311.
9. Kantarjian H, O'Brien S, Cortes J, Wierda W, Faderl S, et al. (2008) Therapeutic advances in leukemia and myelodysplastic syndrome over the past 40 years. Cancer 113: 1933–1952.
10. Tallman MS (2004) Acute promyelocytic leukemia as a paradigm for targeted therapy. Semin Hematol 41: 27–32.
11. Druker BJ (2008) Translation of the Philadelphia chromosome into therapy for CML. Blood 112: 4808–4817.
12. Grant S (2008) Is the focus moving toward a combination of targeted drugs? Best Pract Res Clin Haematol 21: 629–637.
13. Ashburn TT, Thor KB (2004) Drug repositioning: identifying and developing new uses for existing drugs. Nat Rev Drug Discov 3: 673–683.
14. Chong CR, Sullivan DJ, Jr. (2007) New uses for old drugs. Nature 448: 645–646.
15. Bunce CM, Mountford JC, French PJ, Mole DJ, Durham J, et al. (1996) Potentiation of myeloid differentiation by anti-inflammatory agents, by steroids and by retinoic acid involves a single intracellular target, probably an enzyme of the aldoketoreductase family. Biochim Biophys Acta 1311: 189–198.
16. Scatena R, Nocca G, Sole PD, Rumi C, Puggioni P, et al. (1999) Bezafibrate as differentiating factor of human myeloid leukemia cells. Cell Death Differ 6: 781–787.
17. Nilsson A, Farrants AK, Nesland JM, Finstad HS, Pedersen JI (1995) Potentiating effects of clofibric acid on the differentiation of HL-60 human promyelocytic leukemia cells induced by retinoids. Eur J Cell Biol 67: 379–385.
18. Tiziani S, Lodi A, Khanim FL, Viant MR, Bunce CM, et al. (2009) Metabolomic profiling of drug responses in acute myeloid leukaemia cell lines. PLoS ONE 4: e4251.
19. Fenton SL, Luong QT, Sarafeim A, Mustard KJ, Pound J, et al. (2003) Fibrates and medroxyprogesterone acetate induce apoptosis of primary Burkitt's lymphoma cells and cell lines: potential for applying old drugs to a new disease. Leukemia 17: 568–575.
20. Hayden RE, Pratt G, Davies NJ, Khanim FL, Birtwistle J, et al. (2009) Treatment of primary CLL cells with bezafibrate and medroxyprogesterone acetate induces apoptosis and represses the pro-proliferative signal of CD40-ligand, in part through increased 15dDelta12,14,PGJ2. Leukemia 23: 292–304.
21. Ray DM, Akbiyik F, Phipps RP (2006) The peroxisome proliferator-activated receptor gamma (PPARgamma) ligands 15-deoxy-Delta12,14-prostaglandin J2 and ciglitazone induce human B lymphocyte and B cell lymphoma apoptosis by PPARgamma-independent mechanisms. J Immunol 177: 5068–5076.
22. Morosetti R, Servidei T, Mirabella M, Rutella S, Mangiola A, et al. (2004) The PPARgamma ligands PGJ2 and rosiglitazone show a differential ability to inhibit proliferation and to induce apoptosis and differentiation of human glioblastoma cell lines. Int J Oncol 25: 493–502.
23. Date M, Fukuchi K, Morita S, Takahashi H, Ohura K (2003) 15-Deoxy-delta12,14-prostaglandin J2, a ligand for peroxisome proliferators-activated receptor-gamma, induces apoptosis in human hepatoma cells. Liver Int 23: 460–466.
24. Hayashi N, Nakamori S, Hiraoka N, Tsujie M, Xundi X, et al. (2004) Antitumor effects of peroxisome proliferator activate receptor gamma ligands on anaplastic thyroid carcinoma. Int J Oncol 24: 89–95.
25. Nikitakis NG, Siavash H, Hebert C, Reynolds MA, Hamburger AW, et al. (2002) 15-PGJ2, but not thiazolidinediones, inhibits cell growth, induces apoptosis, and causes downregulation of Stat3 in human oral SCCa cells. Br J Cancer 87: 1396–1403.
26. Lin MS, Chen WC, Bai X, Wang YD (2007) Activation of peroxisome proliferator-activated receptor gamma inhibits cell growth via apoptosis and arrest of the cell cycle in human colorectal cancer. J Dig Dis 8: 82–88.
27. Kondo M, Shibata T, Kumagai T, Osawa T, Shibata N, et al. (2002) 15-Deoxy-Delta(12,14)-prostaglandin J(2): the endogenous electrophile that induces neuronal apoptosis. Proc Natl Acad Sci U S A 99: 7367–7372.
28. Desmond JC, Mountford JC, Drayson MT, Walker EA, Hewison M, et al. (2003) The aldo-keto reductase AKR1C3 is a novel suppressor of cell differentiation that provides a plausible target for the non-cyclooxygenase-dependent antineoplastic actions of nonsteroidal anti-inflammatory drugs. Cancer Res 63: 505–512.
29. Moriai M, Tsuji N, Kobayashi D, Kuribayashi K, Watanabe N (2009) Down-regulation of hTERT expression plays an important role in 15-deoxy-Delta12,14-prostaglandin J2-induced apoptosis in cancer cells. Int J Oncol 34: 1363–1372.
30. Rossi A, Kapahi P, Natoli G, Takahashi T, Chen Y, et al. (2000) Anti-inflammatory cyclopentenone prostaglandins are direct inhibitors of IkappaB kinase. Nature 403: 103–108.
31. Straus DS, Pascual G, Li M, Welch JS, Ricote M, et al. (2000) 15-deoxy-delta 12,14-prostaglandin J2 inhibits multiple steps in the NF-kappa B signaling pathway. Proc Natl Acad Sci U S A 97: 4844–4849.
32. Stamatakis K, Sanchez-Gomez FJ, Perez-Sala D (2006) Identification of novel protein targets for modification by 15-deoxy-Delta12,14-prostaglandin J2 in mesangial cells reveals multiple interactions with the cytoskeleton. J Am Soc Nephrol 17: 89–98.
33. Sanchez-Gomez FJ, Gayarre J, Avellano MI, Perez-Sala D (2007) Direct evidence for the covalent modification of glutathione-S-transferase P1-1 by electrophilic prostaglandins: implications for enzyme inactivation and cell survival. Arch Biochem Biophys 457: 150–159.
34. Landar A, Shiva S, Levonen AL, Oh JY, Zaragoza C, et al. (2006) Induction of the permeability transition and cytochrome c release by 15-deoxy-Delta12,14-prostaglandin J2 in mitochondria. Biochem J 394: 185–195.
35. Aldini G, Carini M, Vistoli G, Shibata T, Kusano Y, et al. (2007) Identification of actin as a 15-deoxy-Delta12,14-prostaglandin J2 target in neuroblastoma cells: mass spectrometric, computational, and functional approaches to investigate the effect on cytoskeletal derangement. Biochemistry 46: 2707–2718.
36. Perez-Sala D, Cernuda-Morollon E, Canada FJ (2003) Molecular basis for the direct inhibition of AP-1 DNA binding by 15-deoxy-Delta 12,14-prostaglandin J2. J Biol Chem 278: 51251–51260.
37. Kalantari P, Narayan V, Henderson AJ, Prabhu KS (2009) 15-Deoxy-{Delta}12,14-prostaglandin J2 inhibits HIV-1 transactivating protein, Tat, through covalent modification. FASEB J.
38. Renedo M, Gayarre J, Garcia-Dominguez CA, Perez-Rodriguez A, Prieto A, et al. (2007) Modification and activation of Ras proteins by electrophilic prostanoids with different structure are site-selective. Biochemistry 46: 6607–6616.
39. Oh JY, Giles N, Landar A, Darley-Usmar V (2008) Accumulation of 15-deoxy-delta(12,14)-prostaglandin J2 adduct formation with Keap1 over time: effects on potency for intracellular antioxidant defence induction. Biochem J 411: 297–306.
40. Scher JU, Pillinger MH (2005) 15d-PGJ2: the anti-inflammatory prostaglandin? Clin Immunol 114: 100–109.
41. Shibata T, Kondo M, Osawa T, Shibata N, Kobayashi M, et al. (2002) 15-deoxy-delta 12,14-prostaglandin J2. A prostaglandin D2 metabolite generated during inflammatory processes. J Biol Chem 277: 10459–10466.
42. Mills KI, Gilkes AF, Sweeney M, Choudhry MA, Woodgate LJ, et al. (1998) Identification of a retinoic acid responsive aldoketoreductase expressed in HL60 leukaemic cells. FEBS Lett 440: 158–162.
43. Nagase T, Miyajima N, Tanaka A, Sazuka T, Seki N, et al. (1995) Prediction of the coding sequences of unidentified human genes. III. The coding sequences of 40 new genes (KIAA0081-KIAA0120) deduced by analysis of cDNA clones from human cell line KG-1. DNA Res 2: 37–43.
44. Birtwistle J, Hayden RE, Khanim FL, Green RM, Pearce C, et al. (2009) The aldo-keto reductase AKR1C3 contributes to 7,12-dimethylbenz(a)anthracene-3,4-dihydrodiol mediated oxidative DNA damage in myeloid cells: implications for leukemogenesis. Mutat Res 662: 67–74.
45. Penning TM, Sharp RB, Krieger NR (1985) Purification and properties of 3 alpha-hydroxysteroid dehydrogenase from rat brain cytosol. Inhibition by nonsteroidal anti-inflammatory drugs and progestins. J Biol Chem 260: 15266–15272.
46. Lin SX, Shi R, Qiu W, Azzi A, Zhu DW, et al. (2006) Structural basis of the multispecificity demonstrated by 17beta-hydroxysteroid dehydrogenase types 1 and 5. Mol Cell Endocrinol 248: 38–46.
47. Scatena R, Bottoni P, Vincenzoni F, Messana I, Martorana GE, et al. (2003) Bezafibrate induces a mitochondrial derangement in human cell lines: a PPAR-independent mechanism for a peroxisome proliferator. Chem Res Toxicol 16: 1440–1447.
48. Scatena R, Bottoni P, Martorana GE, Ferrari F, De Sole P, et al. (2004) Mitochondrial respiratory chain dysfunction, a non-receptor-mediated effect of synthetic PPAR-ligands: biochemical and pharmacological implications. Biochem Biophys Res Commun 319: 967–973.
49. Giles H, Leff P (1988) The biology and pharmacology of PGD2. Prostaglandins 35: 277–300.
50. Gao L, Zackert WE, Hasford JJ, Danekis ME, Milne GL, et al. (2003) Formation of prostaglandins E2 and D2 via the isoprostane pathway: a mechanism for the generation of bioactive prostaglandins independent of cyclooxygenase. J Biol Chem 278: 28479–28489.
51. Montuschi P, Barnes P, Roberts LJ, 2nd (2007) Insights into oxidative stress: the isoprostanes. Curr Med Chem 14: 703–717.
52. Kim HS, Lee JH, Kim IK (1996) Intracellular glutathione level modulates the induction of apoptosis by delta 12-prostaglandin J2. Prostaglandins 51: 413–425.
53. Brunoldi EM, Zanoni G, Vidari G, Sasi S, Freeman ML, et al. (2007) Cyclopentenone prostaglandin, 15-deoxy-Delta12,14-PGJ2, is metabolized by HepG2 cells via conjugation with glutathione. Chem Res Toxicol 20: 1528–1535.
54. Cox B, Murphey LJ, Zackert WE, Chinery R, Graves-Deal R, et al. (2002) Human colorectal cancer cells efficiently conjugate the cyclopentenone prostaglandin, prostaglandin J(2), to glutathione. Biochim Biophys Acta 1584: 37–45.

55. Paumi CM, Wright M, Townsend AJ, Morrow CS (2003) Multidrug resistance protein (MRP) 1 and MRP3 attenuate cytotoxic and transactivating effects of the cyclopentenone prostaglandin, 15-deoxy-Delta(12,14)prostaglandin J2 in MCF7 breast cancer cells. Biochemistry 42: 5429–5437.
56. Kliewer SA, Lenhard JM, Willson TM, Patel I, Morris DC, et al. (1995) A prostaglandin J2 metabolite binds peroxisome proliferator-activated receptor gamma and promotes adipocyte differentiation. Cell 83: 813–819.
57. Forman BM, Tontonoz P, Chen J, Brun RP, Spiegelman BM, et al. (1995) 15-Deoxy-delta 12, 14-prostaglandin J2 is a ligand for the adipocyte determination factor PPAR gamma. Cell 83: 803–812.
58. Fenton SL, Drayson MT, Hewison M, Vickers E, Brown G, et al. (1999) Clofibric acid: a potential therapeutic agent in AML and MDS. Br J Haematol 105: 448–451.
59. Breitkreutz I, Anderson KC (2008) Thalidomide in multiple myeloma–clinical trials and aspects of drug metabolism and toxicity. Expert Opin Drug Metab Toxicol 4: 973–985.
60. Kuendgen A, Gattermann N (2007) Valproic acid for the treatment of myeloid malignancies. Cancer 110: 943–954.
61. Tallman MS (2008) The expanding role of arsenic in acute promyelocytic leukemia. Semin Hematol 45: S25–29.
62. Hasegawa H, Yamada Y, Komiyama K, Hayashi M, Ishibashi M, et al. (2007) A novel natural compound, a cycloanthranilylproline derivative (Fuligocandin B), sensitizes leukemia cells to apoptosis induced by tumor necrosis factor related apoptosis-inducing ligand (TRAIL) through 15-deoxy-Delta 12, 14 prostaglandin J2 production. Blood 110: 1664–1674.
63. Stamatakis K, Perez-Sala D (2006) Prostanoids with cyclopentenone structure as tools for the characterization of electrophilic lipid-protein interactomes. Ann N Y Acad Sci 1091: 548–570.
64. Milne GL, Musiek ES, Morrow JD (2005) The cyclopentenone (A2/J2) isoprostanes–unique, highly reactive products of arachidonate peroxidation. Antioxid Redox Signal 7: 210–220.
65. Fedotcheva NI, Sokolov AP, Kondrashova MN (2006) Nonezymatic formation of succinate in mitochondria under oxidative stress. Free Radic Biol Med 41: 56–64.
66. Mailloux RJ, Beriault R, Lemire J, Singh R, Chenier DR, et al. (2007) The tricarboxylic acid cycle, an ancient metabolic network with a novel twist. PLoS ONE 2: e690.
67. Schumacker PT (2006) Reactive oxygen species in cancer cells: live by the sword, die by the sword. Cancer Cell 10: 175–176.
68. Lovering AL, Ride JP, Bunce CM, Desmond JC, Cummings SM, et al. (2004) Crystal structures of prostaglandin D(2) 11-ketoreductase (AKR1C3) in complex with the nonsteroidal anti-inflammatory drugs flufenamic acid and indomethacin. Cancer Res 64: 1802–1810.
69. Hodges NJ, Green RM, Chipman JK, Graham M (2007) Induction of DNA strand breaks and oxidative stress in HeLa cells by ethanol is dependent on CYP2E1 expression. Mutagenesis 22: 189–194.